RadioGraphics

Lesions of the Hypothalamus: MR Imaging Diagnostic Features[1]

Sahar N. Saleem, MD, PhD • Ahmed-Hesham M. Said, MD, PhD
Donald H. Lee, MD

CME FEATURE

See accompanying test at http://www.rsna.org/education/rg_cme.html

LEARNING OBJECTIVES FOR TEST 5

After reading this article and taking the test, the reader will be able to:

- Describe the MR imaging anatomy of the hypothalamus.
- Recognize the clinical manifestations and key MR imaging features of various hypothalamic lesions.
- Discuss the MR imaging differential diagnosis for hypothalamic lesions and the potential role of diffusion-weighted imaging and MR spectroscopy in establishing the diagnosis.

TEACHING POINTS

See last page

The hypothalamus is susceptible to involvement by a variety of processes, including developmental abnormalities, primary tumors of the central nervous system (CNS), vascular tumors, systemic tumors affecting the CNS, and inflammatory and granulomatous diseases. The hypothalamus may also be involved by lesions arising from surrounding structures such as the pituitary gland. Magnetic resonance (MR) imaging is the modality of choice for evaluating the anatomy and pathologic conditions of the hypothalamus. The MR imaging differential diagnosis depends on accurate anatomic localization and tissue characterization of hypothalamic lesions through the recognition of their signal intensity and contrast material enhancement patterns. Diffusion-weighted imaging and proton MR spectroscopy can be helpful in differentiating among various types of hypothalamic lesions. Key MR imaging features, in addition to the patient's age and clinical findings at presentation, may be helpful in developing the differential diagnosis for lesions involving the hypothalamic region.

Abbreviations: CNS = central nervous system, CSF = cerebrospinal fluid, DI = diabetes insipidus, EPP = ectopic posterior pituitary, FLAIR = fluid-attenuated inversion recovery, LCH = Langerhans cell histiocytosis, MT = mamillothalamic tract, NF = neurofibromatosis, RCC = Rathke cleft cyst

RadioGraphics 2007; 27:1087–1108 • **Published online** 10.1148/rg.274065123 • **Content Codes:** MR NR

[1]From the Department of Diagnostic Radiology, Faculty of Medicine, Cairo University-Kasr Al Ainy Hospital, 4 St 49 Mokattam, Cairo 11451, Egypt (S.N.S.); the Department of Diagnostic Radiology, Faculty of Medicine, Beny-Suif University, Beny-Suif, Egypt (A-H.M.S.); and the Department of Diagnostic Radiology, London Health Sciences Centre, University of Western Ontario, London, Ontario, Canada (D.H.L.). Recipient of a Certificate of Merit award for an education exhibit at the 2005 RSNA Annual Meeting. Received June 23, 2006; revision requested September 7 and received October 16; accepted October 18. All authors have no financial relationships to disclose. **Address correspondence to** S.N.S. (e-mail: *saharsaleem1@gmail.com*).

Figure 1. **(a)** Drawing shows the hypothalamus (outlined with a dashed line) lying below an imaginary line between the anterior commissure *(AC)* and the posterior commissure *(PC)*. The anterior boundary of the hypothalamus is the lamina terminalis *(LT)*, which extends between the optic chiasm *(OC)* and the anterior commissure. The posterior boundary is imprecise; it is indicated by a line that extends between the mamillary bodies *(MB)* and the posterior commissure. The floor of the hypothalamus is formed by the infundibular stalk *(IS)*, the tuber cinereum *(TC)*, and the mamillary bodies. The major tracts related to the hypothalamus, the mamillothalamic tract *(MT)* and the postcommissural fornix *(PF)*, are also shown. **(b)** Sagittal T1-weighted MR image clearly demonstrates the anatomy of the hypothalamus. Note the high-signal-intensity area (arrowhead) representing the posterior pituitary gland. *AC* = anterior commissure, *IS* = infundibular stalk, *LT* = lamina terminalis, *MB* = mamillary bodies, *OC* = optic chiasm, *PC* = posterior commissure, *TC* = tuber cinereum. **(c)** On a sagittal contrast material–enhanced MR image, the infundibular stalk and pituitary gland show normal homogeneous enhancement, which reflects their lack of a blood-brain barrier.

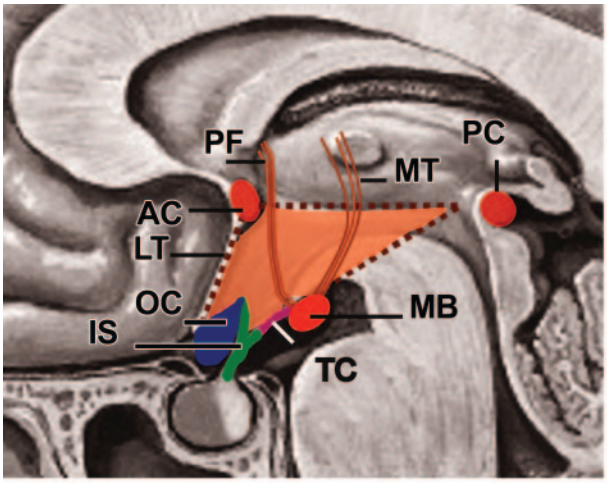

a.

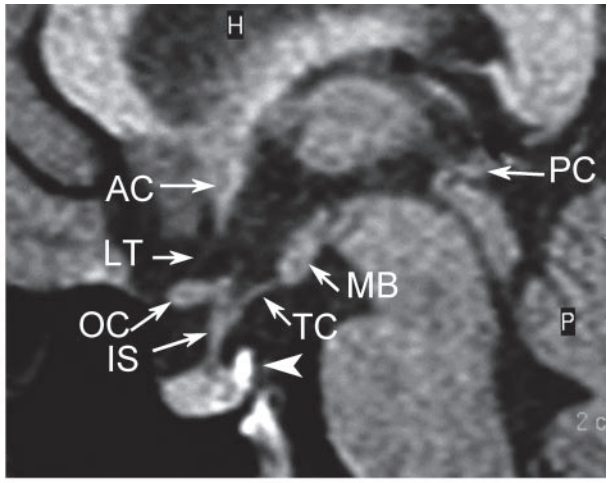

b.

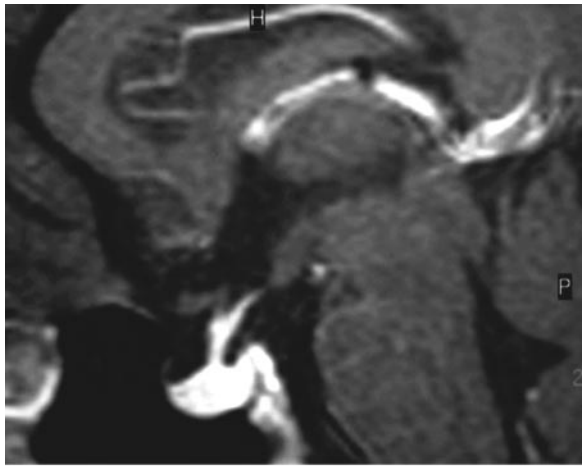

c.

Introduction

The hypothalamus (from the Greek *hypo*, meaning "below," and *thalamus*, meaning "bed") is that part of the diencephalon located below the thalamus. It is a small but highly complex structure in the brain that controls many important body functions (1–4). Magnetic resonance (MR) imaging is the modality of choice in evaluating the hypothalamic region (5–11).

In this article, we review the development, gross anatomy, and function of the hypothalamus; MR imaging of the hypothalamus; the anatomy of the hypothalamus at MR imaging; and the classification and clinical manifestations of hypothalamic lesions. In addition, we discuss and illustrate the MR imaging features of these lesions, including developmental abnormalities (craniopharyngioma, germinoma, hamartoma, lipoma, dermoid and epidermoid cysts, Rathke cleft cyst [RCC], colloid cyst), primary tumors of the central nervous system (CNS) (hypothalamic-chiasmatic glioma, ganglioglioma, choristoma), vascular tumors (hemangioblastoma, cavernoma), systemic tumors affecting the CNS, inflammatory and granulomatous diseases (Langerhans cell histiocytosis [LCH], lymphocytic infundibuloneurohypophysitis, sarcoidosis), and lesions arising from surrounding structures (12–18). We also discuss the differential diagnosis for lesions involving the hypothalamus.

Figure 2. Coronal T1-weighted MR images obtained at the level of (from rostral to caudal) the optic chiasm **(a)**, median eminence **(b)**, and mamillary bodies **(c)** show the various hypothalamic structures. The major hypothalamic tracts and nuclei (circled) are arranged symmetrically about the floor and lower medial surface of the third ventricle and include the arcuate nucleus *(A)*, anterior commissure *(AC)*, dorsomedial nucleus *(DM)*, lateral nucleus *(L)*, lateral preoptic nucleus *(LPO)*, mamillary bodies *(MB)*, medial preoptic nucleus *(MPO)*, posterior nucleus *(P)*, paraventricular nucleus *(PV)*, suprachiasmatic nucleus *(SC)*, supraoptic nucleus *(SO)*, and ventromedial nucleus *(VM)*. The arcuate nucleus is located at the base of the infundibulum. *F* = fornix, *ME* = median eminence, *MT* = mamillothalamic tract, *OC* = optic chiasm, *OT* = optic tract.

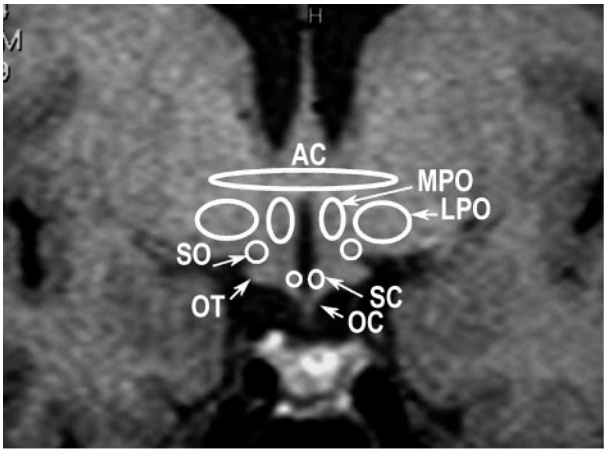

a.

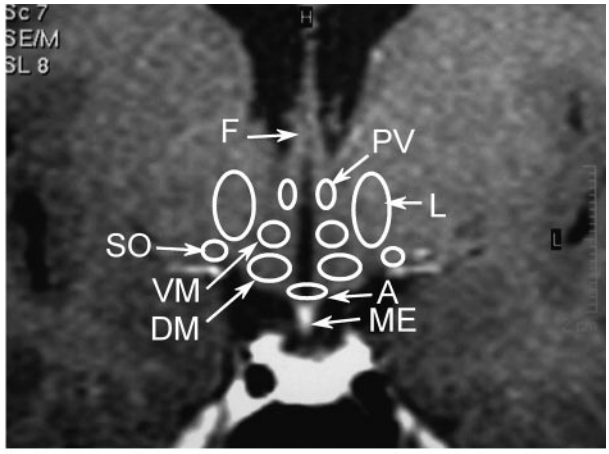

b.

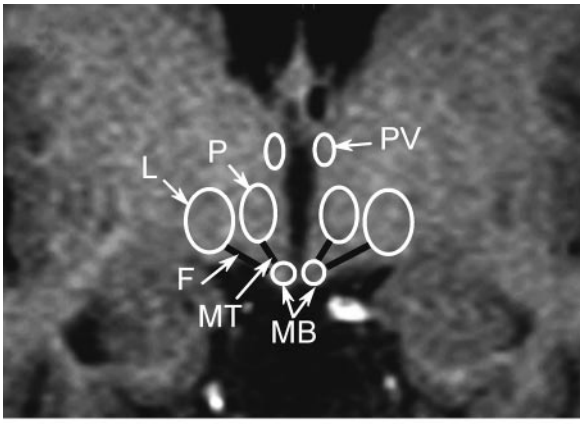

c.

Development of the Hypothalamus

The hypothalamus develops from the neuroectoderm of the floor of the brain, which also forms the posterior pituitary gland. The anterior pituitary gland has a different embryologic origin, deriving from the Rathke pouch from the roof of the mouth (1).

Gross Anatomy of the Hypothalamus

The anterior boundary of the hypothalamus is indicated by a "line" that extends from the anterior commissure to the optic chiasm and corresponds to the lamina terminalis. The posterior boundary of the hypothalamus is indicated by a line that extends from the mamillary bodies to the posterior commissure. This boundary is imprecise because the hypothalamus imperceptibly blends into the mesencephalic tegmentum. The lateral boundary of the hypothalamus is the medial thalamus, and the hypothalamic sulcus separates the hypothalamus from the thalamus superiorly. Inferiorly, the hypothalamus forms the tuber cinereum, a tubular structure that is composed of gray matter and lies between the mamillary bodies posteriorly and the optic chiasm anteriorly. The median eminence is a small bulge in the tuber cinereum that continues downward to form the infundibular stalk, which is attached to the posterior lobe of the pituitary gland (Fig 1) (2–4).

The hypothalamus is composed of a number of nuclei and fiber tracts that are arranged symmetrically about the floor and lower medial surface of the third ventricle. Most of the components of the hypothalamus can be identified on the basis of their location with respect to two axes, the medial-lateral axis and the rostral-caudal axis (Fig 2). As its name implies, the medial-lateral axis divides the hypothalamus into medial and lateral areas. The majority of hypothalamic

Table 1
Locations of Hypothalamic Nuclei with Respect to the Medial-Lateral and Rostral-Caudal Axes

Region*	Medial Area	Lateral Area
Anterior	Medial preoptic nucleus, supraoptic nucleus, paraventricular nucleus, anterior nucleus, suprachiasmatic nucleus	Lateral preoptic nucleus, lateral nucleus, part of supraoptic nucleus
Tuberal	Dorsomedial nucleus, ventromedial nucleus, arcuate nucleus	Lateral nucleus, lateral tuberal nuclei
Posterior	Mamillary nuclei, posterior nucleus	Lateral nucleus

*The rostral-caudal axis divides the hypothalamus into anterior, tuberal, and posterior regions.

nuclei are located medially. The lateral area contains a heterogeneous group of axons called the medial forebrain bundle, which connects the forebrain and the brainstem. The rostral-caudal axis further subdivides the hypothalamus into anterior, tuberal, and posterior regions (Table 1) (3,4).

There are two major white matter tracts in the hypothalamus: the postcommissural fornix and the mamillothalamic tract (MT) (5). The postcommissural fornix extends from each fornical column, runs behind the anterior commissure, and terminates at the mamillary body. The MT arises from the medial mamillary nucleus, passes dorsally, and terminates at the anterior thalamic nuclei, initially forming a well-defined bundle known as the principal mamillary bundle (fasciculus mamillaris princeps) (3). This bundle passes dorsally for a short distance before dividing into two components: a larger MT and a smaller mamillotegmental tract. The MT terminates at the anterior thalamic nuclei (6).

Function of the Hypothalamus

The main function of the hypothalamus is homeostasis. Measurable factors such as blood pressure, body temperature, fluid and electrolyte balance, and body weight are maintained at a precise value called the set point. The hypothalamus does so by regulating three interrelated functions: endocrine secretion, autonomic function, and emotions (7). The hypothalamus controls the release of hormones by the pituitary gland. Secretion from the posterior pituitary gland can occur as a result of direct neuronal stimulation via the infundibulum, whereas secretion from the anterior pituitary gland is dependent upon the portal plexus, a vascular conduit that carries hypothalamic releasing factors to the anterior pituitary gland (1,7).

MR Imaging of the Hypothalamus

Sagittal and coronal spin-echo T1-weighted sequences are performed with thin sections (≤2–3 mm) and a small field of view (16–20 cm). The same sequences can be repeated after the intravenous administration of a standard dose (0.2 mmol/kg) of gadopentetate dimeglumine (8). Sagittal dynamic images may be acquired for the evaluation of hypothalamic lesions after the rapid injection of gadopentetate dimeglumine. Serial images can be obtained every 15 seconds (turbo spin-echo) or 30 seconds (conventional spin-echo) for 240 seconds after contrast material injection (9). Contrast-enhanced fat-suppressed images can also be useful in assessing the hypothalamic region. Alternatively, a three-dimensional spoiled gradient-echo volume acquisition can be used, resulting in thinner sections (1–1.5 mm) with a good signal-to-noise ratio that can be reconstructed in all three planes. Axial T2-weighted and diffusion-weighted images can be obtained either selectively for the hypothalamic-pituitary axis or for the whole brain. Axial imaging with a fluid-attenuated inversion recovery (FLAIR) sequence, as well as sagittal, coronal, or axial imaging with a constructive interference in steady state sequence, may be used to depict the cerebrospinal fluid (CSF) or lesions with fluidlike contents such as arachnoid or epidermoid cysts (10). MR angiography is a useful tool that can provide most if not all of the necessary vascular information. It may be used to evaluate the adjacent vasculature with larger hypothalamic lesions and to rule out possible aneurysms. In addition to these MR imaging sequences, MR spectroscopy may be performed for further evaluation of a hypothalamic lesion (11).

Table 2
Classification of Hypothalamic Lesions

Pathologic Process	Lesions
Developmental abnormalities	Craniopharyngioma, germinoma, hamartoma, lipoma, dermoid and epidermoid cysts, arachnoid cyst, RCC, colloid cyst
Primary tumors of the CNS	Hypothalamic-chiasmatic glioma, ganglioglioma, choristoma, perisellar meningioma
Vascular tumors	Hemangioblastoma, cavernoma
Systemic tumors affecting the CNS	Metastasis, lymphoma, leukemia
Inflammatory and granulomatous diseases	LCH, lymphocytic infundibuloneurohypophysitis, sarcoidosis, Wegener granulomatosis, tuberculosis, syphilis, encephalitis
Lesions arising from surrounding structures	Suprasellar pituitary tumor, ectopic posterior pituitary (EPP), aneurysms

MR Imaging Anatomy of the Hypothalamus

Teaching Point

Sagittal MR imaging clearly demonstrates the hypothalamic structures from the lamina terminalis and the optic chiasm anteriorly to the mamillary bodies posteriorly. The inferior surface of the hypothalamus between these structures shows the tuber cinereum, the median eminence, and the infundibular stalk (5,6). The infundibulum tapers smoothly as it continues inferiorly from the hypothalamic origin to the pituitary insertion. The normal infundibulum is 3 mm wide at its origin and 2 mm wide near its insertion. The posterior pituitary gland appears as a crescentic hyperintense area on T1-weighted MR images due to lipid in glial cell pituicytes and to phospholipids of vasopressin (Fig 1b). Coronal images help identify the infundibular stalk, optic chiasm, and cavernous sinuses (Fig 2). On contrast-enhanced MR images, the infundibular stalk and pituitary gland show homogeneous contrast enhancement, since they lack a blood-brain barrier (Fig 1c). Although individual hypothalamic nuclear groups cannot be identified with MR imaging, some of the major fiber tracts that traverse the hypothalamus can be seen as low-signal-intensity structures, particularly on T2-weighted images (5,6). These tracts include the fornix, the MT, and, in the most rostral portions of the hypothalamus, the anterior commissure (Fig 2).

Classification of Hypothalamic Lesions

The hypothalamus can be affected by a wide range of lesions. Hypothalamic lesions can extend to involve the surrounding structures, and similarly, the hypothalamus can be involved by lesions affecting the sellar-suprasellar cistern, third ventricle, or thalamus (Table 2) (12–14).

Clinical Manifestations of Hypothalamic Lesions

Patients with hypothalamic lesions may present with hormonal or neurologic disorders due to the direct involvement of the hypothalamus, mass effects of the lesion on the surrounding structures, or both. Lesions arising in the hypothalamus can manifest with any of the following hormonal disorders: diencephalic syndrome, precocious puberty, or hormonal deficiency. Diencephalic syndrome is a rare condition caused by the involvement of the anterior hypothalamus. A child with diencephalic syndrome may present with a history of failure to thrive, vomiting, and emaciation. However, diabetes insipidus (DI) is not usually a feature of this condition, and laboratory tests are usually normal. Lesions involving the tuber cinereum cause oversecretion of gonadotropic hormones, resulting in precocious puberty. For the latter to occur, there must be a functioning tuber cinereum with intact hypothalamic-pituitary pathways; destructive lesions of the hypothalamus or pituitary gland usually do not cause precocious puberty. Hormonal deficiency results in stunted growth and DI.

Epilepsy may be the initial presenting feature in a patient with a hypothalamic lesion. Gelastic seizures (laughing fits) are a specific type of epilepsy that occurs in hypothalamic disease, especially hamartoma of the tuber cinereum (15). Clinical manifestations caused by pressure on the surrounding structures include hydrocephalus,

Table 3
Characteristic Anatomic Locations and Key MR Imaging Features of Hypothalamic Lesions

Lesion	Location	Key MR Imaging Features
Craniopharyngioma	Along suprasellar portion of stalk	Solid and cystic components (solid: heterogeneous enhancement; cystic: variable signal intensity [T1 hyperintensity]), calcification
Germinoma	Upper part of infundibulum	Solid; iso- to hypointense with T1-weighted sequences, iso- to hyperintense with T2-weighted sequences relative to gray matter; contrast enhancement; may be associated with pineal infiltration
Hamartoma	Tuber cinereum	Solid, sometimes with cysts; isointense with T1-weighted sequences, iso- to hyperintense with T2-weighted sequences relative to gray matter; no contrast enhancement or calcification
Osteolipoma	Tuber cinereum	Heterogeneous signal intensity similar to that of fat
Epidermoid cyst	Parasellar	Lobulated borders, isointense with T1- and T2-weighted sequences relative to CSF, hyperintense with FLAIR and diffusion-weighted sequences, no contrast enhancement
Dermoid cyst	Suprasellar, hypothalamic (midline)	Solid, inhomogeneous signal intensity similar to that of fat
Arachnoid cyst	Suprasellar	Isointense relative to CSF, no contrast enhancement
RCC	Supra- or intrasellar	Smooth walls with variable signal intensity, no solid component or calcification
Glioma	Hypothalamic-chiasmic	Solid; hypointense with T1-weighted sequences, hyperintense with T2-weighted sequences; moderately heterogeneous contrast enhancement
Choristoma	Infundibulum	Isointense with T1- and T2-weighted sequences, variable contrast enhancement
Meningioma	Suprasellar (rarely in stalk)	Isointense with T1- and T2-weighted sequences, intense homogeneous contrast enhancement, dural tail
Hemangioblastoma	Hypothalamus	Cyst with enhancing mural nodule
Metastatic disease	Stalk, hypothalamus	Intense contrast enhancement, bone destruction without marked sellar enlargement
LCH	Stalk	Intense contrast enhancement, associated intra- and extracranial lesions
Sarcoidosis	Stalk, suprasellar cistern	Leptomeningeal contrast enhancement, associated intra- and extracranial lesions
Suprasellar pituitary adenoma	Intrasellar center causing upward displacement of optic chiasm	Isointense relative to brain, strong enhancement, may contain cystic component or hemorrhage; sellar enlargement
Suprasellar aneurysm	Suprasellar	Blood products, residual patent lumen, phase artifact

visual disturbances, and pituitary hormonal deficiency (16).

MR Imaging Features of Hypothalamic Lesions

The characteristic anatomic locations and key MR imaging features of hypothalamic lesions are shown in Table 3.

Developmental Abnormalities

Craniopharyngioma.—Craniopharyngiomas derive from remnants of the craniopharyngeal duct. They may arise anywhere along the infundibular stalk from the floor of the third ventricle to the pituitary gland (17). The prevalence of craniopharyngiomas peaks between 10 and 14 years of age, with a second peak occurring in the fourth

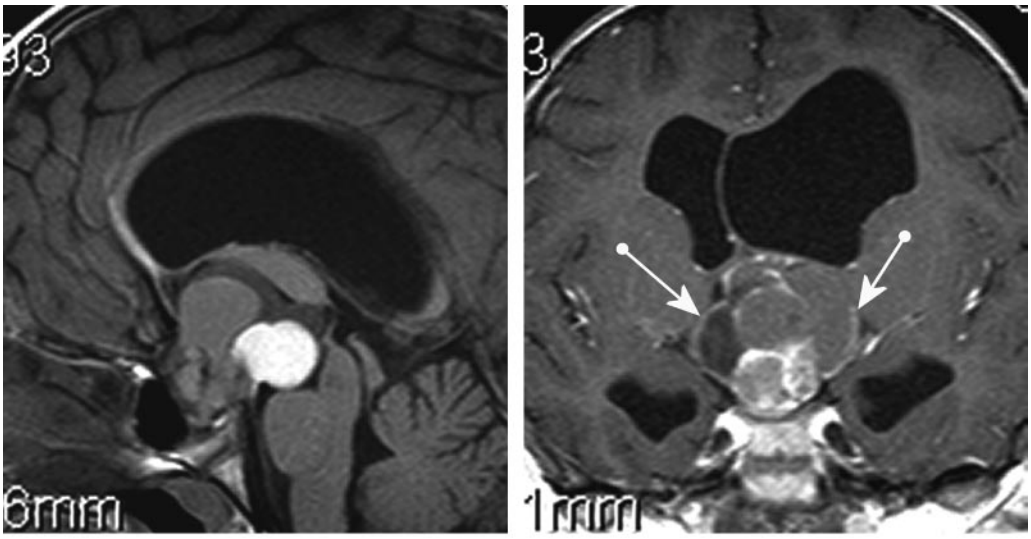

a. b.

Figure 3. Adamantinomatous craniopharyngioma in a 12-year-old boy with headache and blurred vision. Sagittal unenhanced **(a)** and coronal contrast-enhanced **(b)** T1-weighted MR images show a lobulated suprasellar tumor with intrasellar extension. The tumor is formed predominantly of multiple cysts with varying signal intensities that show thin mural contrast enhancement (arrows in **b**). Note the associated asymmetric lateral ventricular dilatation. The diagnosis (adamantinomatous craniopharyngioma) was confirmed at surgery. (Case courtesy of Yasser Ragab, MD, Cairo, Egypt.)

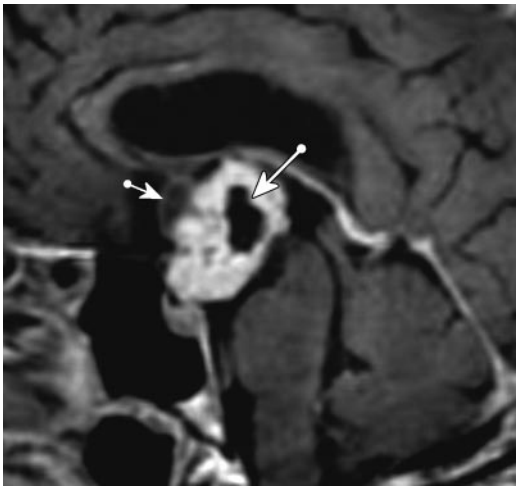

Figure 4. Papillary craniopharyngioma in a 39-year-old man with headache. Sagittal contrast-enhanced T1-weighted MR image shows a predominantly solid, heterogeneously enhancing suprasellar tumor with small, hypointense nonenhancing cystic components (arrows). The diagnosis (papillary craniopharyngioma) was confirmed at surgery.

to sixth decades of life. Males are more commonly affected than females (18). Symptoms typically consist of headaches, visual field defects, and hypothalamic dysfunction (usually DI). Craniopharyngiomas are divided histologically into two types: adamantinomatous (pediatric) and papillary (adult) types. Some tumors have mixed histologic features. Pediatric craniopharyngiomas typically appear at MR imaging as predominantly multicystic suprasellar masses. The cystic areas may be iso-, hyper-, or hypointense relative to brain tissue with T1-weighted sequences. The short T1 relaxation times are the result of very high protein content. With T2-weighted sequences, both the cystic and solid components tend to have high signal intensity. After the administration of contrast material, the solid portions enhance heterogeneously. The thin walls of the cystic areas nearly always enhance (Fig 3). The characteristic calcifications in pediatric craniopharyngiomas may not be discernible, although gradient-echo images may show susceptibility effects from calcified components. Occasionally, craniopharyngiomas are predominantly solid, typically without calcification; these solid tumors usually have papillary histologic features with a heterogeneous appearance and enhancement characteristics.

It has been postulated that lobulated craniopharyngiomas with large, hyperintense cysts on T1-weighted MR images are adamantinomatous, whereas the smaller, round, primarily solid craniopharyngiomas with hypointense cysts on T1-weighted images have papillary histologic features (Fig 4) (17).

Germinoma.—Germinomas are tumors arising from germ cells and most frequently occur during childhood and young adulthood. Although these lesions are most commonly located in the pineal region, they can also occur primarily in the hypothalamic region. Synchronous lesions in the hypothalamic and pineal regions account for 10% of all intracranial germ cell tumors. Hypothalamic germinomas affect males and females with equal frequency and commonly cause symptoms indicative of hypothalamic involvement, such as DI, emaciation, or precocious puberty (18). At MR imaging, germinomas have typical imaging features, appearing as homogeneous, well-marginated round solid masses with gray matter signal intensity that involve the infundibular stalk and the floor of the third ventricle (18). They are iso- to hypointense with T1-weighted sequences and iso- to slightly hyperintense with T2-weighted sequences. The short T2 relaxation time presumably reflects the diminished free water content of these tumors. Contrast enhancement is prominent and homogeneous (Fig 5) (18). Suprasellar germinomas are characterized by homogeneity and the lack of cystic and calcific components. Typically, the high signal intensity of the posterior pituitary lobe will not be seen on sagittal T1-weighted images due to blockage of the infundibulum by the mass. It is important to recognize that at the time a child presents with DI, the hypothalamic germinoma may be small or even not yet visible at radiology. In such patients, brain MR imaging should be performed every 3–6 months during the first 3 years after the onset of DI (19).

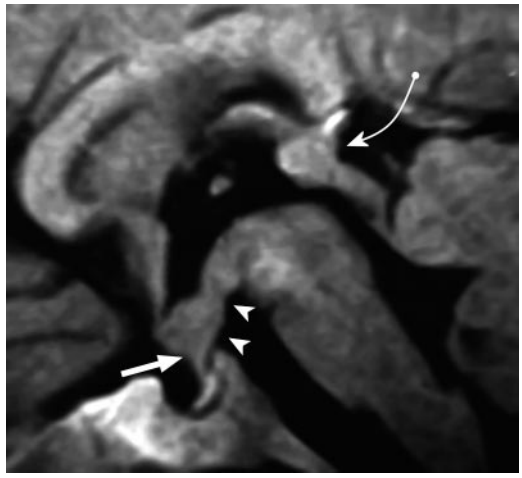

Figure 5. Metachronous hypothalamic and pineal gland germinomas in a 3-year-old girl with central DI. Sagittal contrast-enhanced T1-weighted MR image shows a well-defined, lobulated, homogeneously enhancing mass (germinoma) involving the proximal part of the infundibular stalk (straight arrow) and the base of the hypothalamus (arrowheads). An associated pineal gland germinoma (curved arrow) is also seen. The diagnosis was confirmed at surgery.

Hamartoma.—Hypothalamic hamartomas are developmental malformations consisting of tumorlike masses located in the tuber cinereum of the hypothalamus. Most patients present in the first or second decade of life, with boys being more commonly affected than girls. These lesions have been divided into two main clinicoanatomic subsets: parahypothalamic hamartomas and intrahypothalamic hamartomas. Parahypothalamic hamartomas are pedunculated masses that are attached to the floor of the hypothalamus by a narrow base. These lesions seem more likely to be associated with precocious puberty than with gelastic seizures. Intrahypothalamic hamartomas are sessile masses with a broad attachment to the hypothalamus. They appear to lie within the substance of the hypothalamus itself and may distort the contour of the third ventricle. In addition, they seem to be associated more often with gelastic seizures than with precocious puberty (20). At pathologic analysis, hypothalamic hamartomas contain nerve cells that resemble those of the normal hypothalamus, along with normal glial cells (21). At MR imaging (Fig 6), they are seen as well-defined pedunculated or sessile lesions at the tuber cinereum and are isointense (22) or mildly hypointense (11) on T1-weighted images and iso- to hyperintense on T2-weighted images, with no contrast enhancement or calcification. The absence of any long-term change in the size, shape, or signal intensity of the lesion strongly supports the diagnosis of hypothalamic hamartoma (11,22).

Lipoma.—Intracranial lipomas are uncommon maldevelopmental lesions that tend to involve midline structures such as the infundibulum. Intracranial osteolipomas are very rare, with only about 30 cases having been reported in the literature. Features that help distinguish them from other intracranial lipomas include their *(a)* arrangement of central adipose and peripheral osseous tissues, *(b)* consistent size, and *(c)* consistent location between the mamillary bodies and the infundibular stalk. In contrast, osteolipomas at other intracranial sites are relatively rare (23). In the few reported cases of symptomatic osteolipomas of the tuber cinereum, patients presented with a variety of neurologic symptoms and endocrinologic disturbances such as precocious puberty (24). However, in most of the reported

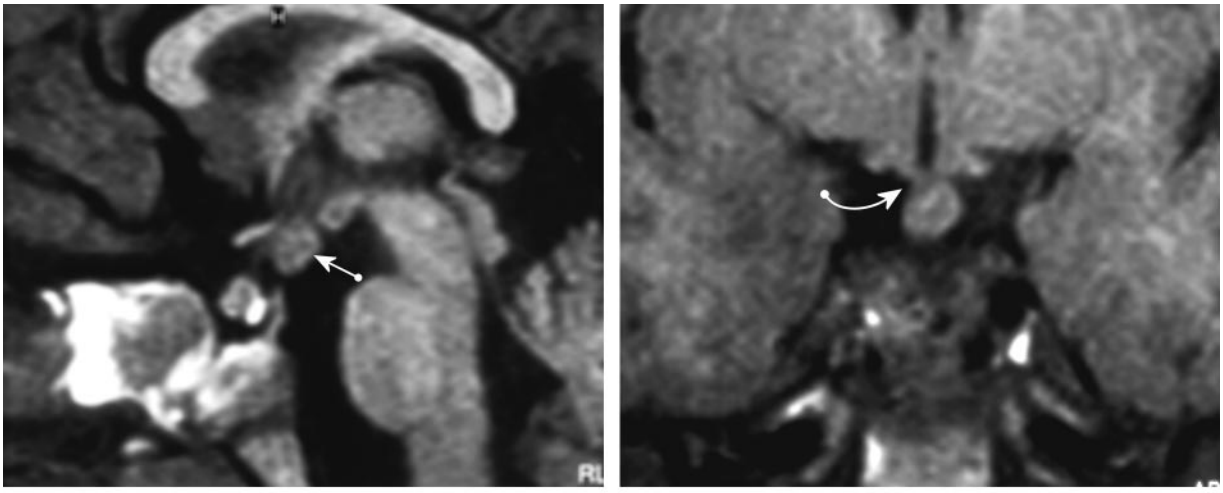

a. b.

Figure 6. Parahypothalamic hamartoma of the tuber cinereum in a 7-year-old boy with precocious puberty. Sagittal **(a)** and coronal **(b)** T1-weighted MR images show a well-defined, isointense pedunculated mass (arrow in **a**) in the characteristic location between the infundibular stalk anteriorly and the mamillary bodies posteriorly. The mass is attached to the floor of the hypothalamus by a narrow base (arrow in **b**) but does not lie within the substance of the hypothalamus. The diagnosis was confirmed at surgery.

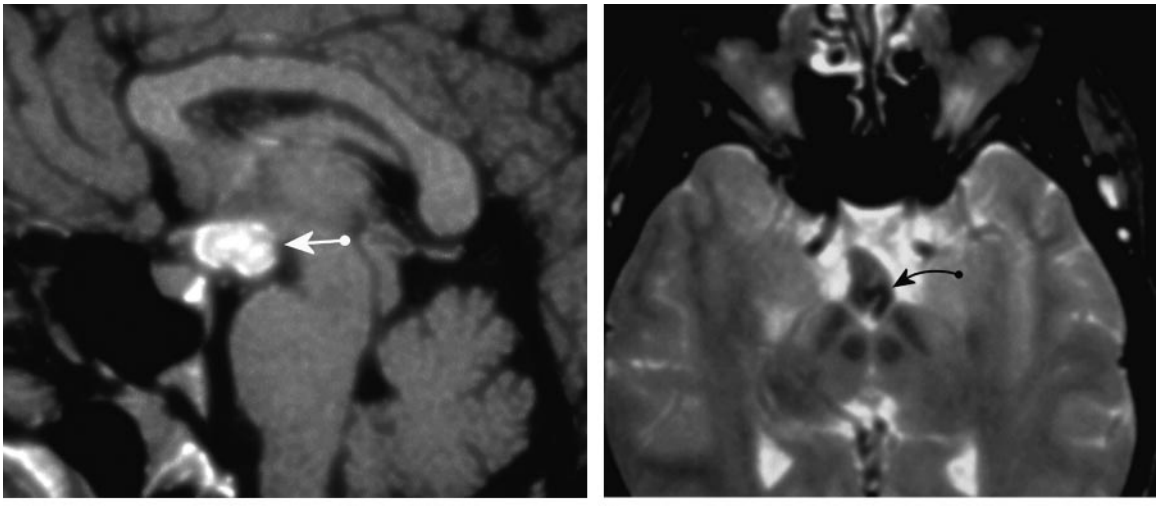

a. b.

Figure 7. Parahypothalamic osteolipoma of the tuber cinereum in a 43-year-old woman with headache and blurred vision. **(a)** Sagittal T1-weighted MR image shows a well-defined high-signal-intensity lesion at the tuber cinereum (arrow). **(b)** On an axial fat-suppressed T2-weighted MR image, the lesion exhibits suppressed signal intensity. Arrow indicates a markedly hypointense linear structure that is consistent with bone tissue, a finding that was confirmed at surgery.

cases, the lesions have been discovered incidentally at autopsy (25). MR imaging of hypothalamic osteolipomas reveals one or more masses located directly behind the infundibular stalk with the signal intensity characteristics of adipose tissue (ie, hyperintense on both T1-weighted and fast spin-echo T2-weighted images, suppressed signal intensity with fat suppression techniques) (Fig 7). Osteolipoma should be included in the radiologic differential diagnosis for hypothalamic masses that demonstrate fat signal intensity and calcification (24).

Dermoid and Epidermoid Cysts.—Dermoid and epidermoid cysts are rare benign maldevelopmental lesions that arise from epithelial inclusions occurring during neural tube closure. Dermoid and epidermoid cysts consist of a capsule composed of epidermal elements, with dermoid cysts containing dermal derivatives (fat, sebaceous glands, hair). Although dermoid and epidermoid cysts are congenital, they usually become

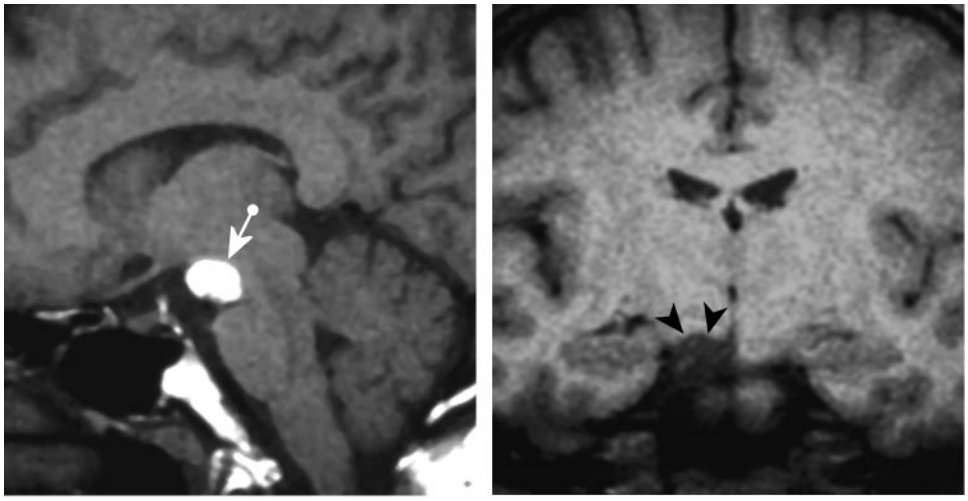

a. b.

Figure 8. Hypothalamic dermoid cyst in a 30-year-old man with headache. **(a)** Sagittal T1-weighted MR image shows a well-defined hyperintense lesion (arrow) at the floor of the hypothalamus posterior to the infundibular stalk. **(b)** On a coronal fat-suppressed T1-weighted MR image, the lesion (arrowheads) exhibits suppressed signal intensity, a finding that indicates adipose contents. The diagnosis (hypothalamic dermoid cyst) was confirmed at surgery.

symptomatic only in early adulthood as a result of the inner accumulation of desquamated cell debris deriving from the capsule. Suprasellar lesions can cause visual abnormalities and endocrinologic disturbances (eg, DI) (26).

Intracranial dermoid cysts are more common than suprasellar dermoid cysts and arise in the midline, most commonly below the tentorium (27). The MR imaging characteristics of dermoid cysts depend on the contents of the lesion. The signal intensity of dermoid cysts is usually like that of fat and may be similar to that of lipomas on both T1- and T2-weighted images. However, with fat-suppressed sequences, lipomas exhibit more signal intensity suppression than do dermoid cysts (Fig 8) (28). Dermoid cysts with low fat content may demonstrate CSF-like signal intensity. Dermoid cysts appear hyperintense relative to CSF on FLAIR images and thus can be differentiated from CSF-containing arachnoid cysts (29).

The location of epidermoid cysts is more variable than that of dermoid cysts and shows greater deviation from the midline. The frequency of occurrence in the parasellar region is surpassed only by that in the cerebellopontine angle cistern (26). On both T1- and T2-weighted MR images, epidermoid cysts are slightly more hyperintense with heterogeneous signal intensity compared with CSF-containing arachnoid cysts. Calcification and contrast enhancement are rare and usually occur at the periphery in epidermoid cysts. With FLAIR and diffusion-weighted pulse sequences, epidermoid cysts show higher signal intensity than does CSF; these sequences, as well as constructive interference in steady state sequences, are essential for defining lesion extent and help differentiate the lesion from an arachnoid cyst or enlarged CSF space (10).

Rathke Cleft Cyst.—RCCs are benign sellar cysts derived from Rathke pouch remnants. They are lined with epithelium and contain mucoid material. In 71% of cases, the cysts are partially intrasellar and partially suprasellar in location (30). Purely suprasellar RCCs with a normal pituitary gland have also been reported (31). Although RCCs are usually asymptomatic, they may produce symptoms by compressing the pituitary gland or hypothalamus, most frequently in patients 50–60 years of age. MR imaging shows a round, sharply defined intra- or suprasellar mass that typically lies anterior to the infundibular stalk. Axial images show the cyst to be located at the junction between the anterior and posterior

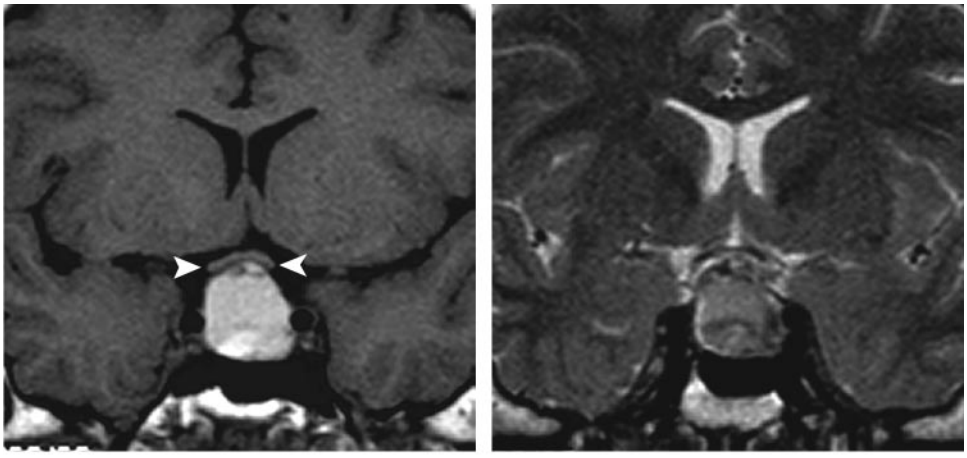

a. b.

Figure 9. RCC in a 50-year-old woman with diplopia. Coronal T1-weighted **(a)** and T2-weighted **(b)** MR images show a well-defined intra- and suprasellar lesion that displaces the optic chiasm upward (arrowheads in **a**). The cystic contents have high signal intensity on the T1-weighted image and low signal intensity on the T2-weighted image, typical findings that indicate a high concentration of mucopolysaccharides (confirmed at surgery). The epicenter of the lesion is sellar. (Case courtesy of Yasser Ragab, MD, Cairo, Egypt.)

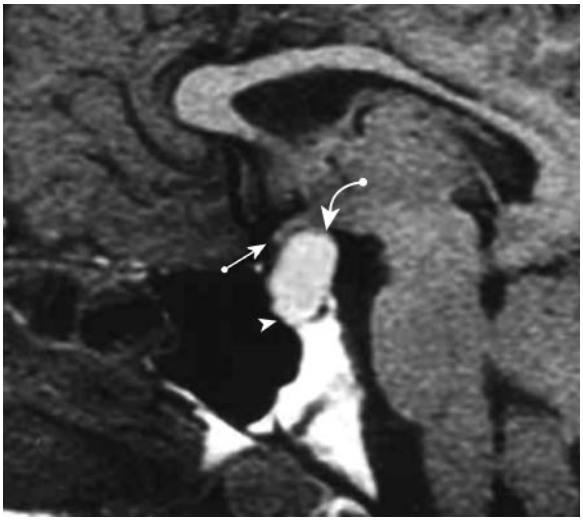

Figure 10. Suprasellar colloid cyst in a 44-year-old man with decreased visual acuity. Sagittal T1-weighted MR image shows a well-defined, homogeneously hyperintense suprasellar cyst (curved arrow) that displaces the optic chiasm upward (straight arrow), with intrasellar extension that compresses the pituitary gland (arrowhead). The cyst also showed homogeneous high signal intensity with T2-weighted sequences. The diagnosis (suprasellar colloid cyst) was confirmed at surgery.

pituitary gland. The cystic contents may have variable signal intensity: either low signal intensity on T1-weighted images and high signal intensity on T2-weighted images resembling CSF, or high signal intensity on T1-weighted images and variable signal intensity on T2-weighted images owing to a high mucopolysaccharide content. Neither contrast enhancement nor calcifications are usually seen (Fig 9) (30,31).

Colloid Cyst.—Colloid cysts are slow-growing lesions, probably of neuroepithelial or endodermal origin. They are usually located in the anterosuperior third ventricle close to the foramen of Monro. Other locations such as the suprasellar cistern have also been reported, albeit rarely. Colloid cysts are typically found in adults, usually in the fifth to sixth decades of life. The most common clinical manifestations of intra- or suprasellar colloid cysts are hypogonadism, galactorrhea, and headache (32). Colloid cysts are lined by a single layer of epithelial cells and are filled with a thick viscous mucus consisting of a variety of ingredients including blood products, macrophages, cholesterol crystals, and numerous metallic ions. The MR imaging signal intensity of colloid cysts is notoriously variable, with myriad combinations of T1 and T2 signal intensities having been described (Fig 10). The most common appearance is hyperintensity on T1-weighted images and iso- to hypointensity on T2-weighted images. Colloid cysts do not show contrast enhancement or calcification (33).

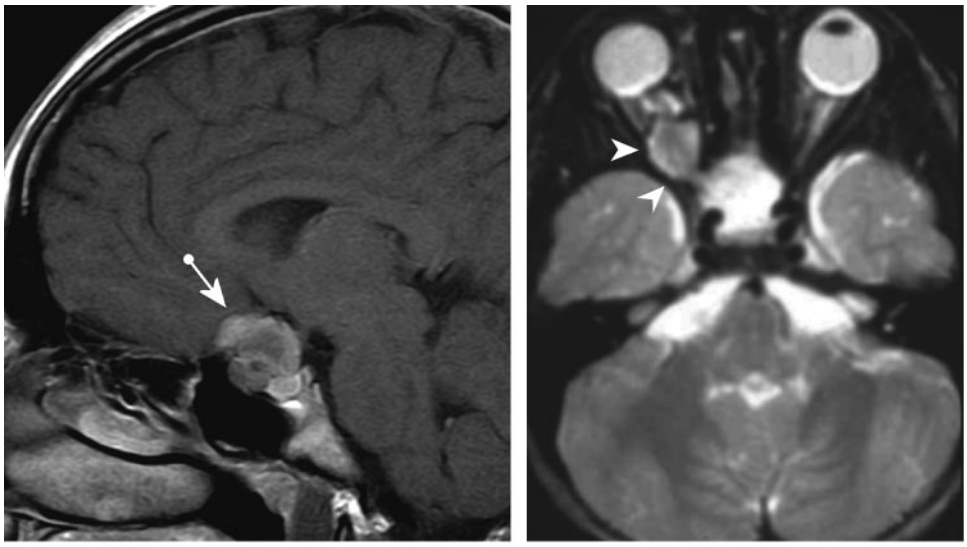

a. b.

Figure 11. Hypothalamic-chiasmatic glioma in a 4-year-old boy with NF-1. Sagittal T1-weighted **(a)** and axial T2-weighted **(b)** MR images show an irregular hypothalamic mass (arrow in **a**) that involves the optic chiasm and extends to the right optic nerve (arrowheads in **b**). The mass has heterogeneous low signal intensity on the T1-weighted image and high signal intensity on the T2-weighted image, findings that are typical for this lesion. The diagnosis (hypothalamic-chiasmatic glioma) was confirmed at surgery.

Primary Tumors of the CNS

Hypothalamic-Chiasmatic Glioma.—Hypothalamic and optic gliomas are discussed together in this article, since the distinction between the two tumor types is arbitrary because the point of origin cannot usually be defined. Gliomas of the optic chiasm and hypothalamus account for 10%–15% of supratentorial tumors in children. Males and females are approximately equally affected. At presentation, patients are usually 2–4 years of age with diminished visual acuity. Endocrine dysfunction, most commonly reduced growth hormone resulting in short stature, is present in about 20% of patients. Between 20% and 50% of patients with hypothalamic gliomas have a positive family history of von Recklinghausen disease (neurofibromatosis [NF]-1) (18). Gliomas of the optic chiasm and hypothalamus in children with NF-1 usually have a more indolent course. Tumors may grow more slowly and occasionally regress spontaneously (34). MR imaging is optimal for showing the relationship of the mass to the hypothalamus, optic chiasm, and infundibulum as well as the intraorbital and intracanalicular components of the mass. Gliomas of the optic chiasm and hypothalamus are almost always hypointense with T1-weighted sequences and hyperintense with T2-weighted and FLAIR sequences (Fig 11). Large tumors are typically heterogeneous with cystic and solid components, with the latter enhancing markedly after contrast material administration (18).

Ganglioglioma.—Gangliogliomas are relatively benign slow-growing tumors composed of mixed nerve and glial cells. They are rare, accounting for only 0.4%–1.3% of all brain tumors, and are most often found in the temporal lobe. Gangliogliomas involving the hypothalamus and optic chiasm are extremely rare. In a review of 11 reported cases of gangliogliomas involving the optic chiasm, the mean patient age was 20 years and the tumor showed a slight male predilection. All of the patients had visual impairment. Secondary hyperprolactinemia from pituitary stalk compression was observed in one case. The MR imaging findings in gangliogliomas are nonspecific. The lesions may be iso- to hypointense on T1-weighted images and hyperintense on T2-weighted images. Cystic components occur in about 60% of gangliogliomas; in the remaining cases, the lesion consists entirely of solid components. The cystic components may show a higher signal intensity than does CSF on T2-weighted images, a finding that represents gelatinous material. Contrast enhancement may have either a nodular rim or solid enhancement pattern (Fig 12) (35).

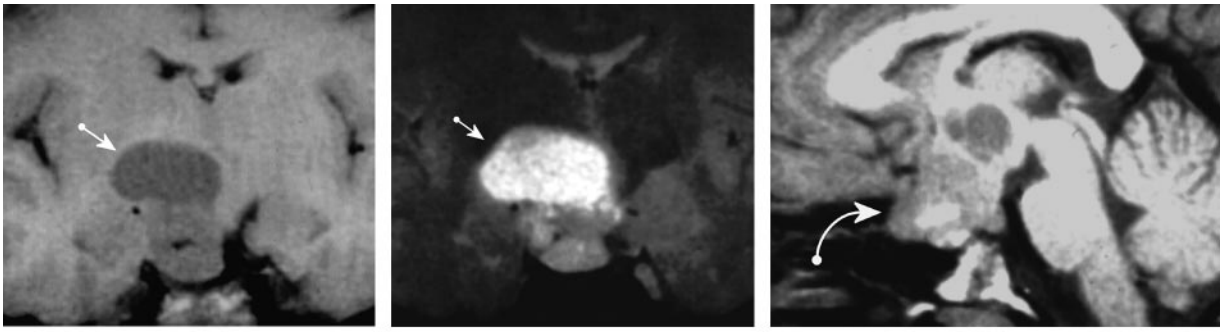

a. b. c.

Figure 12. Hypothalamic ganglioglioma in a 20-year-old man with headache and blurred vision. Coronal contrast-enhanced T1-weighted **(a)** and T2-weighted **(b)** MR images and sagittal contrast-enhanced T1-weighted image **(c)** show an irregular hypothalamic mass with mixed cystic and enhancing solid components (arrow in **c**). The cystic components are hyperintense relative to CSF (arrow in **a** and **b**).

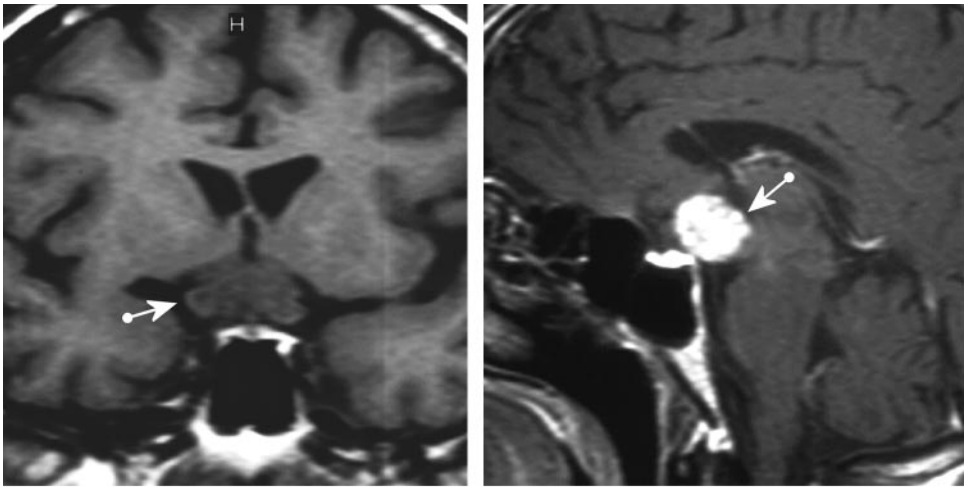

a. b.

Figure 13. Choristoma in a 55-year-old man with gradual diminution of vision. Coronal unenhanced **(a)** and sagittal contrast-enhanced **(b)** T1-weighted MR images show a well-defined suprasellar mass (arrow). The mass is iso- to slightly hypointense relative to the brain on the unenhanced image and shows inhomogeneous enhancement on the contrast-enhanced image.

Choristoma.—Choristomas are distinctive low-grade gliomas arising along the distribution of the neurohypophysis, including both the infundibular stalk and the posterior lobe of the pituitary gland. They are thought to be derived from pituicytes, a modified astrocyte and the principal posterior pituitary cell.

Because of their enigmatic origin, choristomas are also known by various other names, including infundibuloma and granular cell tumor (36–38).

Choristomas are rare tumors; to our knowledge, only about 70 cases have been reported in the literature (36–41). The tumors commonly manifest during the fourth or fifth decade of life and have a female predilection of 2:1. Common clinical findings include visual field defects and endocrinologic disturbances such as panhypopituitarism or, rarely, DI. Choristomas are benign and slow growing with no pronounced tendency for invasion or recurrence (36,37). At MR imaging, choristomas appear as well-defined masses in the suprasellar cistern, in the sella, or in both. The MR imaging signal intensity characteristics vary depending on the presence of cystic components. The solid parts of the tumor are isointense relative to the brain on T1- and T2-weighted images, with inhomogeneous enhancement on contrast-enhanced images (Fig 13) (37).

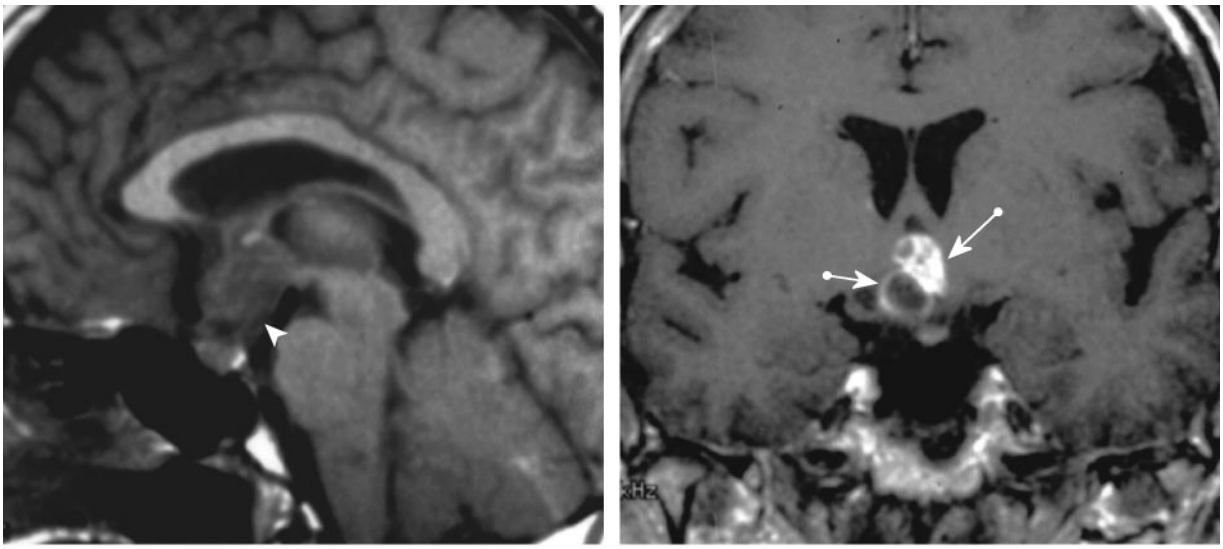

a. b.

Figure 14. Hypothalamic hemangioblastoma in a 54-year-old woman with headache. **(a)** Sagittal T1-weighted MR image shows a heterogeneous, hypointense hypothalamic lesion (arrowhead). **(b)** On a coronal contrast-enhanced T1-weighted MR image, the lesion demonstrates complex cystic components with marginal contrast enhancement (short arrow) and an intensely enhancing mural nodule (long arrow).

Vascular Tumors

Hemangioblastoma.—Hemangioblastomas are benign vascular tumors representing 2% of primary tumors of the CNS. They are most frequently seen in patients between 35 and 45 years of age (42). Although hemangioblastomas are usually isolated tumors, they can also be associated with von Hippel–Lindau disease, a hereditary condition that predisposes patients to hemangioblastomas in the CNS and a variety of visceral tumors (43). Hemangioblastomas in von Hippel–Lindau disease occur in younger patients and have a worse prognosis than do sporadic hemangioblastomas (44). Hemangioblastomas most frequently affect the cerebellum, followed by the spinal cord and the brainstem (43). Tumor location at the hypothalamic-pituitary axis is very unusual, with very few cases having been reported to date. Hemangioblastomas in this location should raise a high degree of suspicion for von Hippel–Lindau disease (44). The best imaging technique available for hemangioblastomas is contrast-enhanced MR imaging (43). Cerebral hemangioblastomas are commonly seen at MR imaging as cystic areas with solid enhancing mural nodules (Fig 14).

Cavernoma.—Cavernous angiomas (cavernomas) are benign vascular malformations that are considered to arise secondary to failure of normal embryonic vascular development. They are most commonly hemispheric and superficial, and in close contact with the subarachnoid space or ventricular system (45). Cavernomas are rarely reported in the hypothalamus, although tumors in this location may be more common in children than in adults (46). MR imaging is the imaging study of choice for parenchymal cavernomas. The characteristic (and diagnostic) imaging findings include a heterogeneous core composed of various stages of hemorrhage, a peripheral rim of low signal intensity representing hemosiderin, and no adjacent edema (Fig 15) (45).

Systemic Tumors Affecting the CNS

Because the tuber cinereum, infundibular stalk, and neurohypophysis lack a blood-brain barrier, they are more vulnerable to hematogenous me-

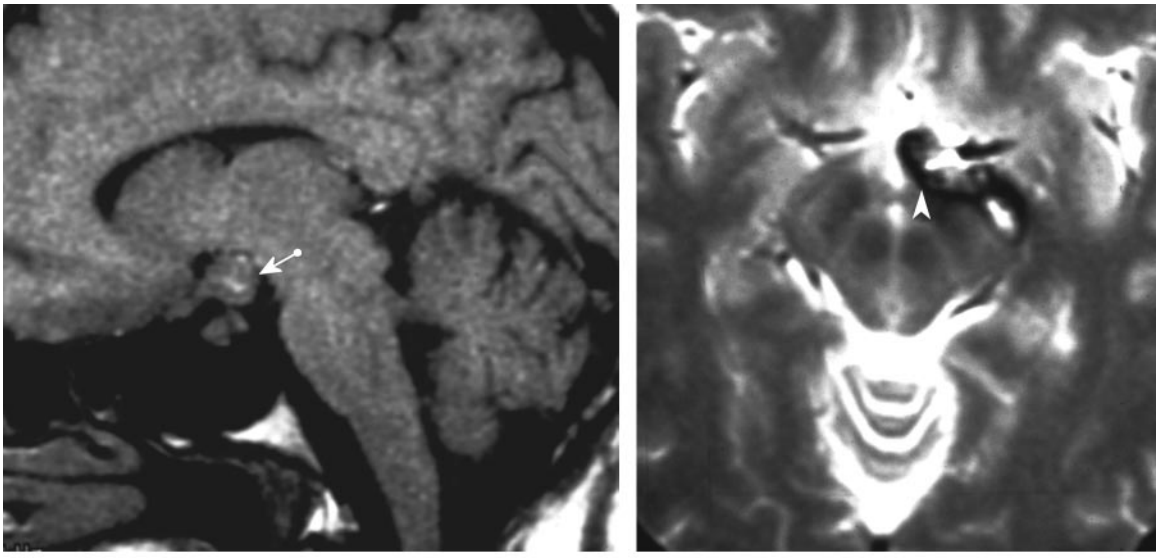

a. b.

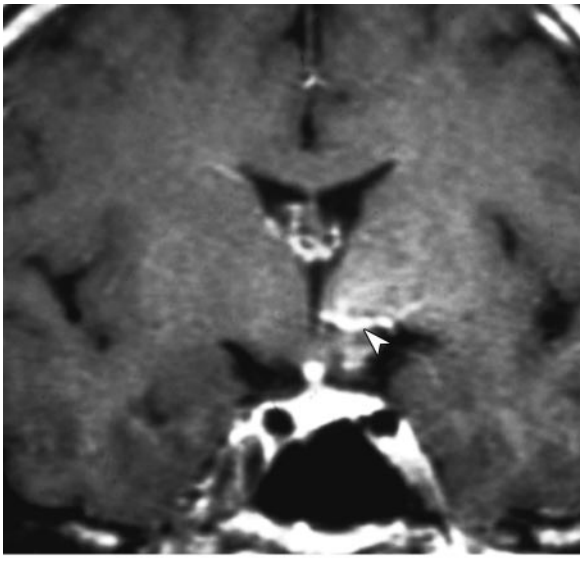

c.

Figure 15. Hypothalamic cavernoma in a 9-year-old boy with acute diminution of vision (chiasmatic apoplexy). **(a)** Sagittal T1-weighted MR image shows a hypothalamic lesion with central hyperintensity (arrow), a finding that indicates hemorrhage. **(b)** Axial T2-weighted MR image shows a signal void (arrowhead) that represents a vascular structure. **(c)** On a coronal contrast-enhanced T1-weighted MR image, the major vein within the lesion (arrowhead) is markedly enhanced and has a typical aberrant transparenchymal course. The MR imaging finding of blood of different ages in a hypothalamic lesion is highly suggestive of cavernoma.

tastasis than is brain parenchyma (47). The frequency of hypothalamic-pituitary axis metastases ranges from 1% to 25% at autopsy in patients with systemic cancer. The most frequent primary site of the tumor in women is the breast, followed by the lung, stomach, and uterus; in men, it is the lung, followed by the prostate gland, urinary bladder, stomach, and pancreas (48). At MR imaging, infundibular metastases cause marked thickening of the stalk. These metastases are usually isointense on T1-weighted images and enhance after contrast material injection (47). Unlike pituitary adenomas, metastases to the hypothalamic-pituitary axis show strong bone destruction without marked sellar enlargement (Fig 16).

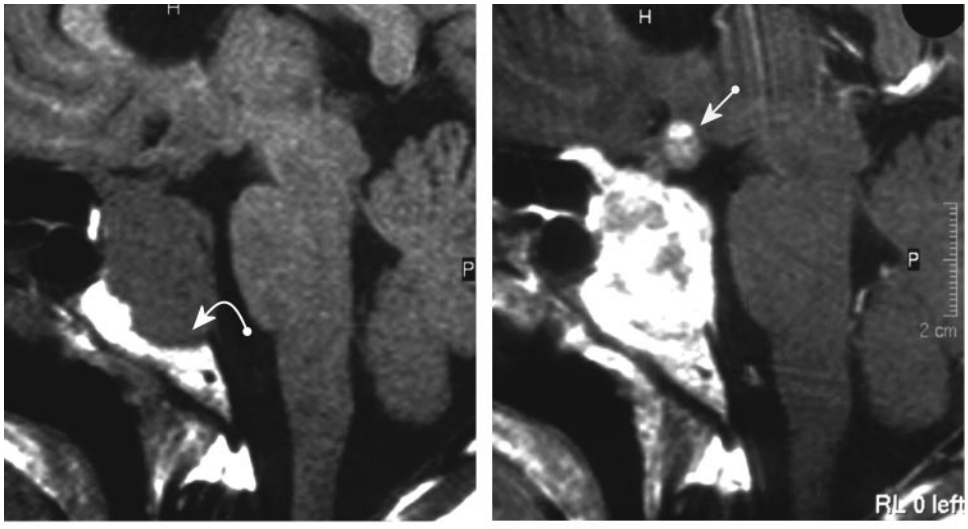

a. b.

Figure 16. Metastatic carcinoma to the hypothalamic-pituitary axis in a 46-year-old woman with breast cancer. **(a)** Sagittal T1-weighted MR image shows a large clival mass with destruction of the sella and invasion of the suprasellar region (arrow). **(b)** Corresponding contrast-enhanced MR image clearly shows extension of the metastatic lesion and depicts a small enhancing hypothalamic mass (arrow).

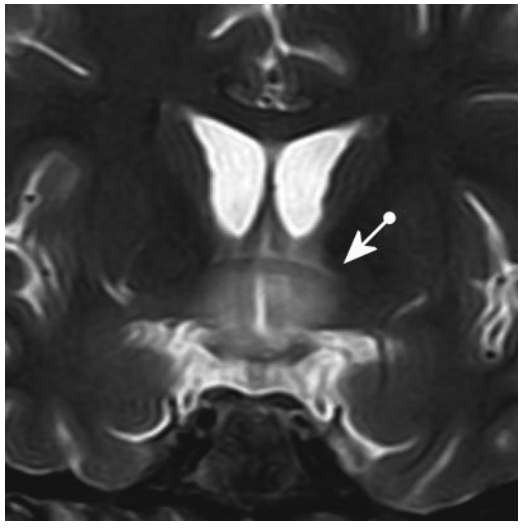

Figure 17. Hypothalamic encephalitis in a 35-year-old man with DI. Coronal T2-weighted MR image reveals a hyperintense area in the thalamic-hypothalamic region (arrow) that corresponds to edematous changes. (Courtesy of Yasser Ragab, MD, Cairo, Egypt.)

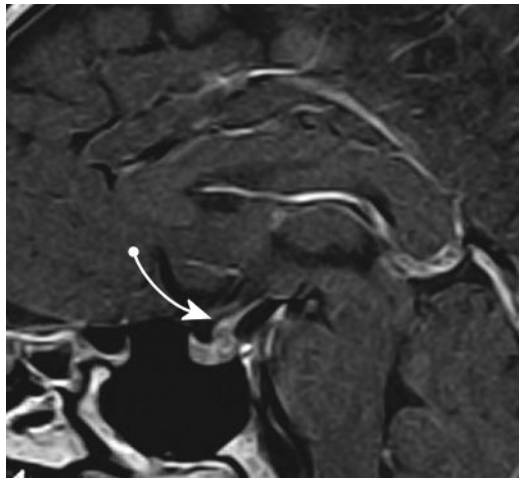

Figure 18. LCH in an 8-year-old boy with DI. Sagittal contrast-enhanced T1-weighted MR image shows a thickened infundibular stalk (arrow). Note that the normal hyperintensity of the posterior pituitary gland is missing. (Courtesy of Yasser Ragab, MD, Cairo, Egypt.)

Inflammatory and Granulomatous Diseases

Encephalitis is inflammation of the brain parenchyma and may have either infectious or noninfectious causes. The most common cause of infectious encephalitis is viral infection. Viral hypothalamic encephalitis may manifest with fever, DI, and the syndrome of inappropriate ADH secretion (49). MR imaging shows the extent of inflammation in the hypothalamus and helps differentiate encephalitis from other hypothalamic conditions manifesting with masses. Edema in the hypothalamus is hyperintense on T2-weighted and FLAIR images and iso- or hypointense on T1-weighted images (Fig 17) (50).

The causes of noninfectious inflammation of the hypothalamus include LCH, lymphocytic infundibulohypophysitis, and sarcoidosis.

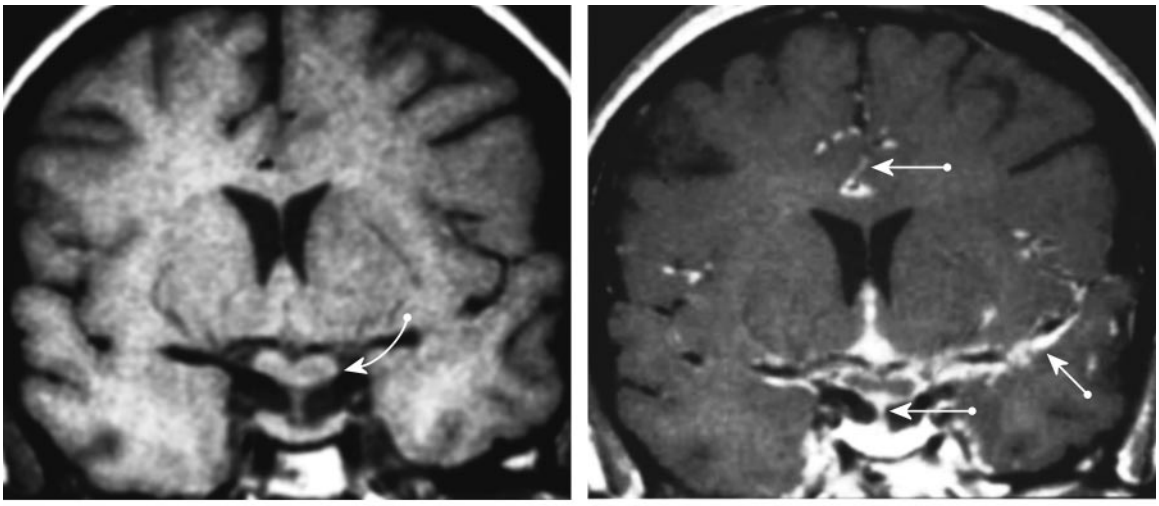

a. b.

Figure 19. Neurosarcoidosis in a 32-year-old woman with DI. **(a)** Coronal unenhanced T1-weighted MR image shows irregular thickening of the optic chiasm (arrow). **(b)** Corresponding contrast-enhanced MR image shows widespread nodular leptomeningeal and infundibular stalk enhancement (arrows). Note that the leptomeningeal granulomas are not visible on the unenhanced image.

Langerhans Cell Histiocytosis.—LCH is a disease that is dominated by Langerhans cells, which are bone marrow–derived cells of the dendritic cell line. These cells are involved in a variety of immune responses and can infiltrate many anatomic sites in the form of localized lesions or manifest as widespread systemic disease. LCH has a prevalence of 0.2–2.0 cases per 100,000 children under 15 years of age; less than 30% of all reported cases involve adults (51). LCH lesions have an unexplained predilection for the hypothalamic-pituitary axis. Hypothalamic involvement results in DI in 5%–50% of LCH patients. At MR imaging, the most frequent morphologic change is thickening (3 mm) of the infundibular stalk (Fig 18). Involvement varies from mild thickening of the infundibular stalk to a frank hypothalamic mass centered in the superior aspect of the stalk. Hypothalamic lesions enhance markedly after the intravenous infusion of contrast material. Loss of the normal hyperintensity of the posterior pituitary gland (bright spot) on T1-weighted images, a partially or completely empty sella, or threadlike narrowing of the infundibulum (maximum width <1 mm) can also be seen in LCH (9,52). Apart from lesions in the hypothalamic-pituitary region, CNS involvement has been reported in only 4% of patients with LCH (51,52).

Lymphocytic Infundibuloneurohypophysitis.—Lymphocytic infundibuloneurohypophysitis is an autoimmune inflammatory condition caused by infiltration primarily of the hypothalamus, infundibulum, and neurohypophysis by lymphocytes and plasma cells. It is a disease of adults, particularly women presenting with hypopituitarism during the peripartum period. MR imaging shows enlargement of the hypothalamus and infundibulum, and sometimes of the pituitary gland itself. The enlarged regions typically show uniform contrast enhancement. The imaging findings are nonspecific, and the diagnosis is best established histologically on the basis of lymphocytic infiltration of the hypothalamus (53).

Sarcoidosis.—Sarcoidosis is a multisystem granulomatous disorder of unknown cause that most commonly affects young adults of both sexes. The most commonly affected organs are the lungs, skin, and lymph nodes. Clinical involvement of the CNS (neurosarcoidosis) occurs in about 10% of affected patients during the course of the disease. Neurosarcoidosis develops primarily in the leptomeninges and may spread along the Virchow-Robin spaces to form intraparenchymal masses. The disease has a predilection for the base of the brain, particularly the hypothalamus and pituitary gland, although any portion of the CNS may be affected (54). Thus, disturbance of the hypothalamic-pituitary axis (with DI and anterior pituitary failure) is the most common feature of neurosarcoidosis (55). At MR imaging, granulomatous infiltration of the dura mater causes plaquelike or nodular thickening that may be noted on the infundibular stalk and optic chiasm (Fig 19). The lesions tend to be isointense relative to gray matter on T1-weighted images

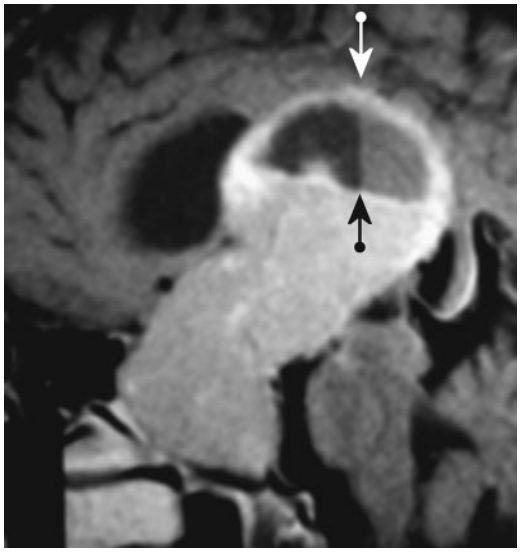

Figure 20. Hemorrhagic pituitary adenoma with a fluid-fluid level in a 42-year-old woman with headache and visual field defects. Sagittal contrast-enhanced T1-weighted MR image shows a large, enhancing, solid sellar and suprasellar tumor. Arrows indicate a fluid-debris level created by the sedimentation of long-standing hemorrhage within the tumor. The diagnosis (hemorrhagic pituitary adenoma) was confirmed at surgery.

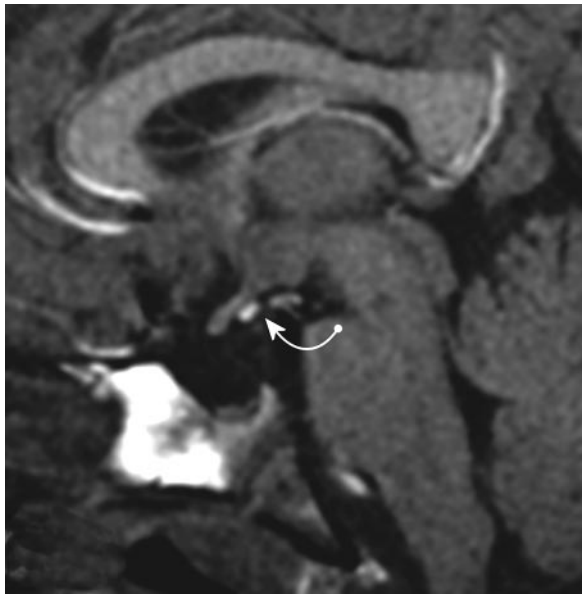

Figure 21. EPP in an 8-year-old boy with growth retardation. Sagittal T1-weighted MR image shows the posterior pituitary gland in an abnormal location at the median eminence and appearing as a small, well-defined area of hyperintensity (arrow). Note that the anterior pituitary gland is small and the infundibular stalk is not visible. (Courtesy of Yasser Ragab, MD, Cairo, Egypt.)

and hypointense on T2-weighted images. However, leptomeningeal granulomas may go unnoticed at unenhanced MR imaging (Fig 19). On gadolinium-enhanced images, intense meningeal enhancement most commonly involves the basal meninges and sulci. One of the most typical manifestations is a thick, enhancing infundibulum (56). Occasionally, granulomas coalesce to form large masslike lesions, particularly in the region of the floor of the third ventricle and optic chiasm (57).

Lesions Arising from Surrounding Structures

Large pituitary adenomas may extend into the suprasellar cistern, invading the hypothalamus (54,58). Ectopic suprasellar pituitary adenomas are very rare (59). At MR imaging, large pituitary adenomas may show variable signal intensity patterns depending on the necrotic, cystic, or hemorrhagic components. The sedimentation of blood products may create fluid-fluid levels within the mass, which are more likely to be observed in pituitary adenomas than in craniopharyngiomas or RCCs (Fig 20) (47,60).

The T1 signal hyperintensity of neurohypophysis is normally seen within the sella. EPP is the presence of this bright signal intensity at another site (eg, the median eminence) (Fig 21) (61). EPP tissue could be due to defective neuronal migration during embryogenesis (61). EPP is commonly associated with attenuation or absence of the infundibular stalk as well as reduced height of the anterior pituitary gland (62).

Differential Diagnosis for Lesions Involving the Hypothalamus

The hypothalamus is susceptible to involvement by a wide variety of pathologic processes. However, the most common masses in the hypothalamic region are suprasellar pituitary adenoma, meningioma, craniopharyngioma, and hypothalamic-chiasmatic glioma; other lesions are less commonly or even rarely seen (47).

Patient age, clinical findings at presentation, and the MR imaging features of lesions involving the hypothalamus may be helpful in developing the differential diagnosis. With regard to patient age, presentation before age 5 years favors the diagnosis of glioma, as does an association with cutaneous or radiologic stigmata of NF-1. Craniopharyngioma, hamartoma, and germinoma are seen in children, whereas RCCs, meningiomas, and inflammatory processes are more common in young adults. Metastatic disease should be

strongly suspected in older patients who present with disease involving the hypothalamus or infundibular stalk (63).

Knowledge of the characteristic clinical manifestations is important in developing a differential diagnosis for hypothalamic lesions. Hamartoma of the tuber cinereum manifests with specific signs and symptoms of precocious puberty or gelastic seizures. Unlike primary pituitary tumors, hypothalamic lesions may cause posterior pituitary failure. DI is usually present at the time of manifestation of hypothalamic germ cell tumors and granulomatous diseases, whereas patients with hypothalamic gliomas rarely develop DI until later in the course of the disease (18). However, in many patients with hypothalamic lesions, the presenting signs and symptoms merely aid in localizing the lesion, and MR imaging features including anatomic location, signal intensity, and contrast enhancement pattern must be considered for a more specific diagnosis.

The excellent anatomic detail at MR imaging facilitates localization of the lesions to the hypothalamus. Some hypothalamic lesions show remarkable consistency in location, such as hamartoma and osteolipoma (in the tuber cinereum) (21,25). A thickened contrast-enhanced infundibulum is the most typical manifestation of germ cell tumors, lymphocytic hypophysitis, sarcoidosis, and LCH (51). However, idiopathic, isolated infundibular stalk thickening can be seen in cases of central DI without evidence of infiltrative processes (64).

Teaching Point

Teaching Point

Involvement of the optic chiasm and optic nerves by hypothalamic tumors may point to the diagnosis of hypothalamic-chiasmatic glioma (22).

Larger hypothalamic lesions may extend into the pituitary fossa and parasellar region. The differential diagnosis for such lesions includes pituitary adenomas with suprasellar extension. Answering the following questions may help in developing a differential diagnosis for a supra- or intrasellar mass.

1. Is the epicenter of the mass suprasellar? The epicenter of primary hypothalamic lesions is suprasellar, whereas that of pituitary adenomas is usually intrasellar.

2. Does the lesion enlarge the sella? An enlarged sella is more compatible with an intrasellar lesion like pituitary adenoma or RCC.

3. Is the lesion extraaxial or intraaxial? Making this determination helps differentiate intraaxial lesions with a hypothalamic origin from extraaxial lesions (eg, meningioma).

4. How are the different structures normally seen in the region affected by the presence of the lesion? Is the optic chiasm displaced upward or downward? Unlike pituitary lesions, hypothalamic masses displace the chiasm downward rather than upward (47,60,65).

MR imaging signal intensity patterns allow the characterization of about 30% of suprasellar lesions (65). Absent signal intensity with all sequences caused by rapidly flowing blood, or absent signal intensity on T1-weighted images with augmentation of signal intensity on T2-weighted images caused by slow or turbulent flow, allows the confident diagnosis of vascular malformations. However, the extremely low signal intensity of a densely calcified lesion can potentially be mistaken for a vascular structure. Gradient-echo images may show susceptibility effects from calcified components (65). T1 signal hyperintensity is a common finding at MR imaging of the hypothalamic region and has different sources. Lesions include EPP; bright signal intensity is related to vasopressin storage in the neurohypophysis. T1 signal hyperintensity may also be related to clotting of blood (hemorrhagic suprasellar pituitary adenoma), a high concentration of protein (RCC, craniopharyngioma), fat (lipoma, dermoid cyst), calcification (craniopharyngioma), or a paramagnetic substance (metastatic melanoma) (60). Many abnormalities involving the hypothalamic region have nonspecific signal intensity characteristics, including gliomas, metastases, and encephalitis, all of which are hypointense on T1-weighted images and hyperintense on T2-weighted images (47,60,65). Lesions of near isointensity relative to the brain include germinomas, some hamartomas, and suprasellar meningioma (19). This isointensity helps differentiate these lesions from other tumors that are typically hyperintense on T2-weighted images (20–22).

Teaching Point

Contrast-enhanced MR imaging findings include a wide variety of enhancement patterns. Classically, hypothalamic hamartomas show no contrast enhancement. This finding is fairly characteristic and is helpful in differentiating hamartomas from other lesions (20).

Enhancement of other hypothalamic lesions ranges from homogeneous (germinoma) to patchy and irregular (craniopharyngioma, glioma) (19,20,22). Associated findings of leptomeningeal enhancement with multiple foci of parenchymal enhancement may point to sarcoidosis (56).

Focal homogeneous enhancement of the infundibular stalk is seen in LCH granulomas (51). Meningiomas may demonstrate an overlying thick

dural enhancement ("dural tail sign") (45). The typical dynamic contrast enhancement pattern of hypothalamic germinomas, LCH, and hemangioblastomas is gradually increasing enhancement without washout, whereas adenohypophysitis demonstrates a sharp rise in enhancement and a steeper washout. Thus, dynamic MR imaging can help distinguish germinomas from adenohypophysitis but is not useful for differentiating them from LCH or hemangioblastomas (66).

Contrast-enhanced MR imaging plays an essential role in differentiating nonneoplastic cysts (eg, arachnoid, epidermoid, and colloid cysts) from cystic neoplasms (eg, RCC, craniopharyngioma, cystic pituitary adenoma) within the hypothalamic region. Unlike nonneoplastic cysts, cystic tumors usually show cyst wall enhancement (67).

Diffusion-weighted pulse sequences are most useful in differentiating epidermoid cysts from arachnoid cysts or enlarged CSF spaces, since epidermoid cysts show higher signal intensity than does CSF (10,17).

Proton MR spectroscopy of hypothalamic gliomas shows increased choline and diminished N-acetyl aspartate. These findings may be useful in differentiating gliomas from craniopharyngiomas, which show a dominant lipid peak (~1 ppm), and from pituitary adenomas, which show only a choline peak or no metabolites at all (68). The presence of lactate and lipid peaks is consistent with aggressive tumors, reflecting anaerobic metabolism and cellular necrosis, respectively. A prominent lipid peak in the MR imaging spectrum of a case of hypothalamic germinoma with seeding suggested its aggressive behavior (69). MR spectroscopy of hypothalamic hamartomas shows a typical pattern of diminished N-acetyl aspartate and increased myoinositol compared with normal gray matter. This signature MR spectroscopic finding associated with hypothalamic hamartomas allows differentiation of these neoplasms from other entities, such as hypothalamic gliomas and metastatic deposits (11).

Teaching Point

References

1. Swaab DF. Disorders of development and growth. In: Swaab DF, ed. The human hypothalamus: basic and clinical aspects. Amsterdam, the Netherlands: Elsevier Health Science, 2004; 31–36.
2. Christ JF. Derivation and boundaries of the hypothalamus, with atlas of hypothalamic grisea. In: Haymaker W, Anderson E, Nauta WJH, eds. The hypothalamus. Springfield, Ill: Thomas, 1969; 13–60.
3. Carpenter MC. Core text of neuroanatomy. 2nd ed. Baltimore, Md: Williams & Wilkins, 1978; 216–235.
4. Gray H. Anatomy of the human body. Philadelphia, Pa: Lea & Febiger, 1918; Bartleby.com, 2000. Available at: http://www.bartleby.com/107/. Accessed March 15, 2006.
5. Saeki N, Sunami K, Kubota M, et al. Heavily T2-weighted MR imaging of white matter tracts in the hypothalamus: normal and pathologic demonstrations. AJNR Am J Neuroradiol 2001;22(8):1468–1475.
6. Miller MJ, Mark LP, Yetkin FZ, et al. Imaging white matter tracts and nuclei of the hypothalamus: an MR-anatomic comparative study. AJNR Am J Neuroradiol 1994;15:117–121.
7. Saper CB, Lowey AD, Swanson LW, Cowan WM. Direct hypothalamo-autonomic connections. Brain Res 1976;117:305–312.
8. Fujii Y, Nakayama N, Nakada T. High-resolution T2 reversed magnetic resonance imaging on a high magnetic field system. J Neurosurg 1998;89:492–495.
9. Maghnie M, Bossi G, Klersy C, Cosi G, Genovese E, Arico M. Dynamic endocrine testing and magnetic resonance imaging in the long-term follow-up of childhood Langerhans cell histiocytosis. J Clin Endocrinol Metab 1998;83:3089–3094.
10. Ikushima I, Korogi Y, Hirai T, et al. MR of epidermoids with a variety of pulse sequences. AJNR Am J Neuroradiol 1997;18(7):1359–1363.
11. Freeman JL, Coleman LT, Wellard RM, et al. MR imaging and spectroscopic study of epileptogenic hypothalamic hamartomas: analysis of 72 cases. AJNR Am J Neuroradiol 2004;25(3):450–462.
12. Laws ER. Brain tumors affecting growth and development. In: Charles GD, Hindmarsh PC, eds. Clinical pediatric endocrinology. Boston, Mass: Blackwell, 2001; 253–258.
13. Ironside JW. Best Practice No 172: pituitary gland pathology. J Clin Pathol 2003;56(8):561–568.
14. Werder K. Pituitary-hypothalamic tumor syndromes: adults. In: Grossman A, ed. Neuroendocrinology, hypothalamus, and pituitary. Available at: http://www.endotext.org/neuroendo/neuroendo11b/neuroendoframe11b.htm. Accessed August 22, 2002.
15. La Rosa C, Stanhope R. Pituitary and hypothalamic tumor syndromes in childhood. In: Grossman A, ed. Neuroendocrinology, hypothalamus, and pituitary. Available at: http://www.endotext.org/neuroendo/index.htm. Accessed August 27, 2003.
16. Molitch ME. Hypothalamic and pituitary tumors: general principles. In: Grossman A, ed. Clinical endocrinology. Boston, Mass: Blackwell, 1998; 129–137.
17. Wasserman JR, Koenigsberg RA. Craniopharyngioma. Emedicine. Available at: http://www.emedicine.com/radio/topic196.htm. Accessed February 23, 2005.

18. Kollias SS, Barkovich AJ, Edwards MS. Magnetic resonance analysis of suprasellar tumors of childhood. Pediatr Neurosurg 1991–1992;17:284–303.
19. Mootha SL, Barkovich AJ, Grumbach MM, et al. Idiopathic hypothalamic diabetes insipidus, pituitary stalk thickening, and the occult intracranial germinoma in children and adolescents. J Clin Endocrinol Metab 1997;82(5):1362–1367.
20. Arita K, Ikawa F, Kurisu K, et al. The relationship between magnetic resonance imaging findings and clinical manifestations of hypothalamic hamartoma. J Neurosurg 1999;91:212–222.
21. Boyko OB, Curnes JT, Oakes WJ, Burger PC. Hamartomas of the tuber cinereum: CT, MR, and pathologic findings. AJNR Am J Neuroradiol 1991;12:309–314.
22. Barkovich AJ. Intracranial, orbital, and neck masses of childhood. In: Barkovich AJ, ed. Pediatric neuroimaging. 4th ed. Philadelphia, Pa: Lippincott Williams & Wilkins, 2005; 573–603.
23. Friede RL. Osteolipomas of the tuber cinereum. Arch Pathol Lab Med 1977;101(7):369–372.
24. Bognar L, Balint K, Bardoczy Z. Symptomatic osteolipoma of the tuber cinereum: case report. J Neurosurg 2002;96(2):361–363.
25. Wittig H, Kasper U, Warich-Kirches M, Dietzmann K, Roessner A. Hypothalamic osteolipoma: a case report. Gen Diagn Pathol 1997;142(5–6):361–364.
26. Caldarelli M, Massimi L, Kondageski C, Di Rocco C. Intracranial midline dermoid and epidermoid cysts in children. J Neurosurg 2004;100(5 suppl pediatrics):473–480.
27. Lunardi P, Missori P. Supratentorial dermoid cysts. J Neurosurg 1991;75:262–266.
28. Feldman RP, Marcovici A, LaSala PA. Intracranial lipoma of the sylvian fissure: case report and review of the literature. J Neurosurg 2001;94(3):515–519.
29. Aprile I, Iaiza F, Lavaroni A, et al. Analysis of cystic intracranial lesions performed with fluid-attenuated inversion recovery MR imaging. AJNR Am J Neuroradiol 1999;20:1259–1267.
30. Voelker JL, Campbell RL, Muller J. Clinical, radiographic, and pathological features of symptomatic Rathke's cleft cysts. J Neurosurg 1991;74(4):535–544.
31. Wenger M, Simko M, Markwalder R, Taub E. An entirely suprasellar Rathke's cleft cyst: case report and review of the literature. J Clin Neurosci 2001;8(6):564–567.
32. Nomikos P, Buchfelder M, Fahlbusch R. Intra- and suprasellar colloid cysts. Pituitary 1999;2(2):123–126.
33. Wagner AL. Brain, colloid cyst. Emedicine. Available at: http://www.emedicine.com/radio/topic96.htm. Accessed February 15, 2005.
34. Allen JC. Initial management of children with hypothalamic and thalamic tumors and the modifying role of neurofibromatosis-1. Pediatr Neurosurg 2000;32(3):154–162.
35. Shuangshoti S, Kirsch E, Bannan P, Fabian VA. Ganglioglioma of the optic chiasm: case report and review of the literature. AJNR Am J Neuroradiol 2000;21(8):1486–1489.
36. Lee CC, Liu CH, Wei CP, How SW. Symptomatic granular cell tumor of the neurohypophysis. J Formos Med Assoc 2004;103(1):58–62.
37. Cohen-Gadol AA, Pichelmann MA, Link MJ, et al. Granular cell tumor of the sellar and suprasellar region: clinicopathologic study of 11 cases and literature review. Mayo Clin Proc 2003;78(5):567–573.
38. Ulm AJ, Yachnis AT, Brat DJ, Rhoton AL Jr. Pituicytoma: report of two cases and clues regarding histogenesis. Neurosurgery 2004;54(3):753–757.
39. Takei H, Goodman JC, Tanaka S, Bhattacharjee MB, Bahrami A, Powell SZ. Pituicytoma incidentally found at autopsy. Pathol Int 2005;55(11):745–749.
40. Kowalski RJ, Prayson RA, Mayberg MR. Pituicytoma. Ann Diagn Pathol 2004;8(5):290–294.
41. Chen KT. Crush cytology of pituicytoma. Diagn Cytopathol 2005;33(4):255–257.
42. Choyke PL, Glenn GM, Walther MM, Patronas NJ, Linehan WM, Zbar B. von Hippel–Lindau disease: genetic, clinical, and imaging features. Radiology 1995;194(3):629–642.
43. Conway JE, Chou D, Clatterbuck RE, et al. Hemangioblastomas of the central nervous system in von Hippel-Lindau syndrome and sporadic disease. Neurosurgery 2001;48(1):55–62.
44. Wasenko JJ, Rodziewicz GS. Suprasellar hemangioblastoma in Von Hippel-Lindau disease: a case report. Clin Imaging 2003;27(1):18–22.
45. Porter PJ, Willinsky RA, Harper W, Wallace MC. Cerebral cavernous malformations: natural history and prognosis after clinical deterioration with or without hemorrhage. J Neurosurg 1997;87(2):190–197.
46. Kurokawa Y, Abiko S, Ikeda N, Ideguchi M, Okamura T. Surgical strategy for cavernous angioma in hypothalamus. J Clin Neurosci 2001;8(suppl 1):106–108.
47. Johnsen DE, Woodruff WW, Allen IS, Cera PJ, Funkhouser GR, Coleman LL. MR imaging of the sellar and juxtasellar regions. RadioGraphics 1991;11:727–758.
48. Schubiger O, Haller D. Metastases to the pituitary-hypothalamic axis: an MR study of 7 symptomatic patients. Neuroradiology 1992;34:131–134.
49. Kastrup O, Wanke I, Maschke M. Neuroimaging of infections. NeuroRx 2005;2(2):324–332.
50. Ishikawa S, Aoki H, Akahane C, et al. Hypothalamic encephalitis with bradycardia. Intern Med 2001;40(8):805–807.
51. Grois N, Prayer D, Prosch H, Lassmann H. CNS LCH Cooperative Group. Neuropathology of CNS disease in Langerhans cell histiocytosis. Brain 2005;128(4):829–838.
52. Prayer D, Grois N, Prosch H, Gadner H, Barkovich AJ. MR imaging presentation of intracranial disease associated with Langerhans cell histiocytosis. AJNR Am J Neuroradiol 2004;25(5):880–891.

53. Honegger J, Fahlbusch R, Bornemann A, et al. Lymphocytic and granulomatous hypophysitis: experience with nine cases. Neurosurgery 1997; 40:713–723.
54. Luk KH, Lam KS, Kung AW, Fung CF, Leung SY. Suprasellar ectopic pituitary adenoma presenting as cranial diabetes insipidus. Postgrad Med J 1992;68(800):467–469.
55. Statement on sarcoidosis. Joint Statement of the American Thoracic Society (ATS), the European Respiratory Society (ERS) and the World Association of Sarcoidosis and Other Granulomatous Disorders (WASOG) adopted by the ATS Board of Directors and by the ERS Executive Committee, February 1999. Am J Respir Crit Care Med 1999; 160(2):736–755.
56. Mana J. Magnetic resonance imaging and nuclear imaging in sarcoidosis. Curr Opin Pulm Med 2002;8(5):457–463.
57. Bakshi R, Fenstermaker RA, Bates VE, Ravichandran TP, Goodloe S Jr, Kinkel WR. Neurosarcoidosis presenting as a large suprasellar mass: magnetic resonance imaging findings. Clin Imaging 1998;22(5):323–326.
58. Horvath E, Kovacs K, Smyth HS, et al. A novel type of pituitary adenoma: morphological features and clinical correlations. J Clin Endocrinol Metab 1988;66:1111–1118.
59. Poussaint TY, Barnes PD, Anthony DC, Spack N, Scott RM, Tarbell NJ. Hemorrhagic pituitary adenomas of adolescence. AJNR Am J Neuroradiol 1996;17(10):1907–1912.
60. Bonneville JF. Pituitary adenomas: value of MR imaging. J Radiol 2000;81(9):939–942.
61. Ultmann MC, Seigel SF, Hirsch WL. Pituitary stalk and ectopic hyperintense T1 signal on magnetic resonance imaging. Am J Dis Child 1993; 147:647–652.
62. Bonneville F, Cattin F, Marsot-Dupuch K, Dormont D, Bonneville JF, Chiras J. T1 signal hyperintensity in the sellar region: spectrum of findings. RadioGraphics 2006;26(1):93–113.
63. Lipscombe L, Asa S, Ezzat S. Management of lesions of the pituitary stalk and hypothalamus. Endocrinologist 2003;13(1):38–51.
64. Leger J, Velasquez A, Garel C, Hassan M, Czernichow P. Thickened pituitary stalk on magnetic resonance imaging in children with central diabetes insipidus. J Clin Endocrinol Metab 1999; 84(6):1954–1960.
65. Lee BC, Deck MD. Sellar and juxtasellar lesion detection with MR. Radiology 1985;157(1):143–147.
66. Liang L, Korogi Y, Sugahara T, et al. Dynamic MR imaging of neurohypophyseal germ cell tumors for differential diagnosis of infundibular diseases. Acta Radiol 2000;41(6):562–566.
67. Hua F, Asato R, Miki Y, et al. Differentiation of suprasellar nonneoplastic cysts from cystic neoplasms by Gd-DTPA MRI. J Comput Assist Tomogr 1992;16(5):744–749.
68. Sutton LN, Wang ZJ, Wehrli SL, et al. Proton spectroscopy of suprasellar tumors in pediatric patients. Neurosurgery 1997;41(2):388–394.
69. Kendi TK, Caglar S, Huvaj S, Bademci G, Kendi M, Alparslan S. Suprasellar germ cell tumor with subarachnoid seeding MRI and MR spectroscopy findings. Clin Imaging 2004;28(6):404–407.

This article meets the criteria for 1.0 credit hour in category 1 of the AMA Physician's Recognition Award. To obtain credit, see accompanying test at http://www.rsna.org/education/rg_cme.html.

RadioGraphics

Lesions of the Hypothalamus: MR Imaging Diagnostic Features

Sahar N. Saleem, MD, PhD et al

RadioGraphics 2007; 27:1087–1108 • **Published online** 10.1148/rg.274065123 • **Content Codes:** MR NR

Page 1091
Sagittal MR imaging clearly demonstrates the hypothalamic structures from the lamina terminalis and the optic chiasm anteriorly to the mamillary bodies posteriorly. The inferior surface of the hypothalamus between these structures shows the tuber cinereum, the median eminence, and the infundibular stalk (5,6).

Page 1105
Some hypothalamic lesions show remarkable consistency in location, such as hamartoma and osteolipoma (in the tuber cinereum) (21,25).

Page 1105
A thickened contrast-enhanced infundibulum is the most typical manifestation of germ cell tumors, lymphocytic hypophysitis, sarcoidosis, and LCH (51). However, idiopathic, isolated infundibular stalk thickening can be seen in cases of central DI without evidence of infiltrative processes (64).

Page 1105
Lesions of near isointensity relative to the brain include germinomas, some hamartomas, and suprasellar meningioma (19).

Page 1106
This signature MR spectroscopic finding associated with hypothalamic hamartomas allows differentiation of these neoplasms from other entities, such as hypothalamic gliomas and metastatic deposits (11).